MINIBOONE STATUS

D.W. Schmitz for the MiniBooNE Collaboration [a]
Columbia University Department of Physics,
538 W 120th St., New York, NY 10027, USA

Neutrino oscillations in the solar and atmospheric Δm^2 regions are now well established. A third region at high Δm^2 has been probed by accelerator-based experiments and a positive signal was reported by the LSND collaboration at Los Alamos [1]. A large Δm^2 neutrino oscillation in addition to the solar and atmospheric results is incompatible with three Standard Model neutrinos, but the LSND result awaits confirmation. The Mini Booster Neutrino Experiment at Fermilab has been designed to confirm or refute the high Δm^2 neutrino oscillations seen by LSND.

1 Introduction

Oscillations of solar and atmospheric neutrinos have been conclusively established by multiple experiments [2]. In addition, oscillations have been seen in accelerator-based neutrino beams and nuclear reactor neutrino experiments designed to search the solar and atmospheric oscillation regions [3].

To understand how to proceed in the neutrino sector, the question of large Δm^2 neutrino oscillations must be settled. The best fit values for solar, atmospheric and LSND oscillations are $\Delta m^2_{solar} \approx 7 \times 10^{-5}\ eV^2$, $\Delta m^2_{atmo} \approx 2.5 \times 10^{-3}\ eV^2$, and $\Delta m^2_{LSND} \approx 0.3 - 3\ eV^2$. Three independent mass squared differences cannot be accommodated by the three weakly interacting neutrinos of the Standard Model. Therefore, the inclusion of the LSND oscillation result implies new physics, and a number of theoretical models have been proposed to explain the experimental results [4].

MiniBooNE has been designed to search this high Δm^2 oscillation region and definitively confirm or refute the result of the LSND experiment.

2 MiniBooNE Overview

The MiniBooNE detector is located 541 m from a neutrino source on the Booster neutrino beam line at Fermi National Accelerator Laboratory. The mean neutrino energy is ~1 GeV, resulting in an $\langle L/E \rangle$ of about 0.5 meters/MeV. This gives MiniBooNE a similar $\langle L/E \rangle$ to LSND (~30m/40MeV), making the experiment sensitive to the same range of oscillations, but with significantly different systematics.

[a] See http://www-boone-fnal.gov/cgi-bin/collaboration/ for entire collaboration list.

2.1 Neutrino Beam

To create the MiniBooNE neutrino beam, 8 GeV kinetic energy protons are taken from the Fermilab Booster and impinged on a 71 cm beryllium target. MiniBooNE has received over 3.6×10^{20} protons on target since September, 2002, and recorded over 380,000 neutrino event candidates in that time.

The target sits inside a magnetic horn used to focus mesons in the direction of the MiniBooNE detector and acts to increase neutrino fluxes by a factor of $\sim$6. MiniBooNE is capable of running in "anti-neutrino mode" by reversing the polarity of the horn power supplies. Currently the experiment is running in neutrino mode; positively charged secondary mesons, predominantly pions and kaons, are focused into a 50 m open cavity and allowed to decay. The neutrino flux at the detector is $\sim$99.5% $\nu_\mu(\overline{\nu_\mu})$ with a small $\nu_e(\overline{\nu_e})$ contamination from K and μ decay.

2.2 MiniBooNE Detector

The MiniBooNE detector is a 6.1 m radius carbon steel sphere filled with 950,000 liters of mineral oil. There are 1280 inward-facing photomultiplier tubes (PMTs) and 240 additional tubes in an optically isolated outer shell used to veto events not originating within the tank. Particle identification is achieved using both prompt Čerenkov light and a small amount of delayed scintillation light. A more detailed description of event selection and energy calibration of the detector can be found elsewhere [5].

3 Charged Current Quasi-Elastic Events and Oscillation Sensitivity

Charged current quasi-elastic (CCQE) events involve a neutrino of flavor l weakly interacting with a nucleon to produce a final state lepton, $\nu_l + n \to p + l^-$. Quasi-elastic kinematics allow the precise measurement of the neutrino energy in these interactions. Based on Monte Carlo studies, MiniBooNE has $\sim$10% energy resolution at 1 GeV assuming no backgrounds. The energy and angle of the lepton with respect to the beam are measured using the charge deposited in the PMTs, and the neutrino energy is reconstructed from $E_\nu = (1/2)(2ME_l - m_l^2)/(M - E_l + cos\theta_l\sqrt{E_l^2 - m_l^2})$ where M is the nucleon mass and E_l, m_l, and θ_l are the lepton energy, mass, and angle, respectively. The visible energy, angle, and reconstructed neutrino energy are shown for data and Monte Carlo in Fig. 1 for ν_μ CCQE events. The curves are unit area normalized. The discrepancy in the highest $\cos\theta$ bin is suspected to be due to unmodeled nuclear effects and is still under study. Also the error bands on these distributions should be significantly reduced with further improvements in the analysis. Both *in situ* and *ex situ* measurements are currently in progress for reducing both beam and detector related uncertainties.

A similar reconstruction method will be applied to identified electrons in the data for performing a $\nu_\mu \to \nu_e$ oscillation search. The MiniBooNE ν_e appearance search is a "blind" analysis, however; the ν_e event spectra will only be analyzed once the analysis is fully matured.

Nevertheless, we can determine the oscillation sensitivity based on projected final statistics and systematic errors. ν_e CCQE events suffer from significantly larger backgrounds than ν_μ events due to mis-identification of other particle types and intrinsic ν_e's in the beam. Assuming the average LSND oscillation probability, MiniBooNE would see $\sim$300 signal ν_e's on top of $\sim$350 misidentified ν_μ CCQE and π^0 events and $\sim$350 background events from intrinsic ν_e's with 1×10^{21} protons on target. The oscillation sensitivity, based on an energy spectrum analysis and assuming 5-10% systematic errors on each background, is shown in Fig 2. Fig. 3 shows the ability to discern a high (1.0 eV^2) *vs.* a low (0.4 eV^2) Δm^2 oscillation parameter with 1×10^{21} protons on target.

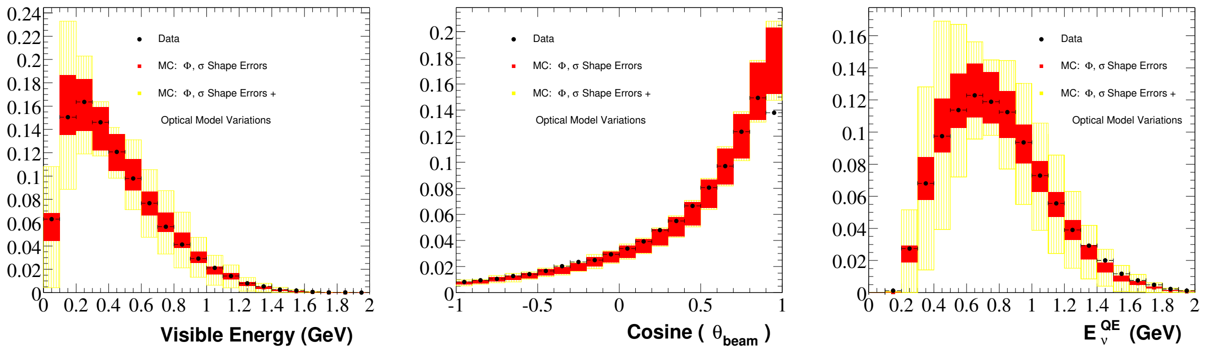

Figure 1: Preliminary data and Monte Carlo reconstructed visible energy (left), cosine of the angle of the lepton w.r.t. the neutrino direction (center), and reconstructed neutrino energy (right) for ν_μ CCQE events. All curves are unit area normalized. The red error bars are flux and neutrino cross section errors added in quadrature. The yellow bands are flux and cross section errors and fluctuations due to typical oil optical model variations added in quadrature.

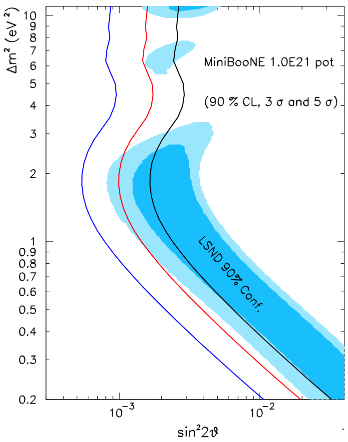

Figure 2: MiniBooNE $\nu_\mu \to \nu_e$ oscillation sensitivity at 90% C.L., 3σ, and 5σ coverage of the LSND allowed region in $(\sin^2 2\theta, \Delta m^2)$ space.

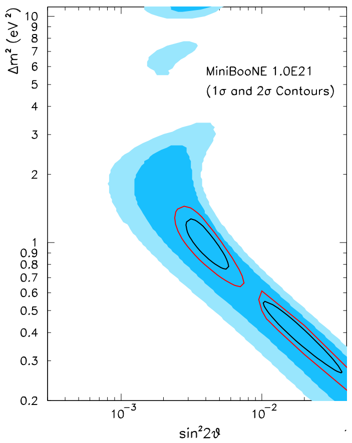

Figure 3: MiniBooNE $\nu_\mu \to \nu_e$ oscillation parameter measurement ability at 1σ and 2σ for a low and high Δm^2 value within the LSND allowed region.

4 Constraining Flux Estimates at HARP

In order to reduce the systematic uncertainties on the neutrino flux at MiniBooNE, the collaboration has cooperated with the Hadron Production Experiment [6] (HARP) at CERN to measure meson production rates directly from the MiniBooNE target. Data were taken in August, 2002, using a 5% interaction length (λ) beryllium disk, a 50% λ and a 100% λ replica MiniBooNE target. The incident beam energy was tuned to match that of the Fermilab Booster at 8 GeV kinetic energy.

Targets used at HARP are positioned inside of a time-projection-chamber (TPC) allowing particle identification over a full 4π of hadron phase space. A first analysis using only the forward PID detectors is currently being performed. This includes a time-of-flight system with ≈180 ps resolution, a Čerenkov detector with a pion threshold of 2.6 GeV/c, and a calorimeter system for separating electrons from hadrons at all momenta. Fig. 4 shows the MiniBooNE neutrino flux as a function of parent pion momentum and angle at production on the MiniBooNE target from the current GEANT4 based MiniBooNE beam Monte Carlo. The gray shaded region shows the pion phase space that is covered by an analysis of the HARP data that includes only the forward particle identification detectors. This "forward" analysis provides excellent coverage of the kinematic range important for MiniBooNE.

Inclusive charged pion cross sections are currently being extracted from the thin target data set. Future analyses will focus on the MiniBooNE replica target data sets to quantify the effects of pion reinteraction in the target. This will provide valuable input to further constraining the ν_μ flux for MiniBooNE. Also, using the time-of-flight and Čerenkov systems, charged kaons should be separable from pions and protons. Studying kaon production from the MiniBooNE target at HARP will constrain background levels of intrinsic ν_e's in the beam from kaon decay.

The analysis of the HARP data sets is currently in progress and will significantly reduce systematic errors on both the predicted ν_μ flux from π^+ decay as well as intrinsic ν_e rates in the beam from K and μ decay.

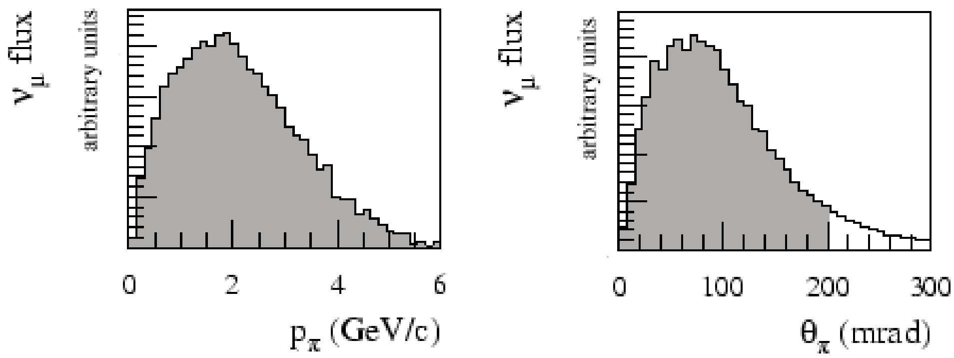

Figure 4: Neutrino fluxes at the MiniBooNE detector shown *vs.* pion phase space variables: momentum (left) and production angle (right). The shaded region indicates the range of acceptance for the HARP PID forward detectors.

Acknowledgments

MiniBooNE gratefully acknowledges the support it receives from the Department of Energy and from the National Science Foundation. The presenter of this paper was supported by NSF grant PHY-98-13383.

References

1. A. Aguilar *et al.*, Phys. Rev. **D64**, 112007 (2001).
2. R. Davis, Prog. Part. Nucl. Phys. **32**, 13 (1994); W. Hampel *et al.*, Phys. Lett. **B447**, 127 (1999); M.B. Smy *et al.*, Phys. Rev. **D69**, 011104 (2004); J. N. Abdurashitov *et al.*, Phys. Lett. **B328**, 234 (1994); Q. R. Ahmad *et al.*, Phys. Rev. Lett. **89**, 011302 (2002); Y. Fukuda *et al.* Phys. Rev. Lett. **81**, 1562 (1998).
3. K. Eguchi *et al.*, Phys. Rev. Lett. **90**, 021802 (2003); M. H. Ahn *et al.*, Phys. Rev. Lett. **90**, 041801 (2003).
4. R. Fardon, A.E. Nelson, and N. Weiner, arXiv:astro-ph/0309800; M. Sorel, J. Conrad, and M. Shaevitz, hep-ph/0305255; G. Barenboim and J. Lykken, Phys. Lett. **B554**, 73 (2003); G. Barenboim and J. Lykken, arXiv:hep-ph/0303238; S. Pakvasa, arXiv:hep-ph/0110175; G. Barenboim, L. Borissov, and J. Lykken, arXiv:hep-ph/0212116.
5. J. Monroe, Proceedings of Rencontres de Moriond 2004, [arXiv:hep-ex/0406048].
6. See G. Vidal, these Proceedings.